Radially symmetric nonlinear photonic crystals

Noa Voloch,* Tal Ellenbogen, and Ady Arie

School of Electrical Engineering, Department of Physical Electronics, Fleishman Faculty of Engineering, Tel Aviv University, Tel Aviv 69978, Israel
**Corresponding author: noavoloc@post.tau.ac.il*

Received July 23, 2008; accepted September 23, 2008;
posted October 16, 2008 (Doc. ID 99186); published December 15, 2008

Different types of quadratic, radially symmetric, nonlinear photonic crystals are presented. The modulation of the nonlinear coefficient may be a periodic or an aperiodic function of the radial coordinate, whereas the azimuthal symmetry of the crystal may be either continuous or discrete. Nonlinear interactions within these structures are studied in two orientations, transverse and longitudinal, for which the interacting beams propagate either perpendicularly or in the plane of modulation. We show that radially symmetric structures can phase match multiple arbitrary processes in any direction. We study multiple wavelength three-wave mixing interactions and multiple direction interactions and analyze spatially dependent polarization states of the generated harmonics. © 2009 Optical Society of America

OCIS codes: 190.4360, 190.2620, 190.4160.

1. INTRODUCTION

Frequency conversion processes resulting from second-order nonlinearity are usually inefficient due to dispersion. The interacting light beams travel with different phase velocities, so intensity fails to build through their propagation path. Efficient construction of output beams can be achieved by a birefringence technique when the wave vector differences between three mixed waves—input pump beam, signal, and idler output beams—is $\mathbf{\Delta k}=\mathbf{k_s}+\mathbf{k_i}-\mathbf{k_p}=0$.

However, it also can be obtained by a quasi-phase-matching (QPM) [1] technique for which the sign of the nonlinear coefficient is modulated periodically or aperiodically along the propagation path of the optical beams. This is realized by one-dimensional (1D) [2] or two-dimensional (2D) [3] domain poling of ferroelectrics. The obtained structures are quadratic nonlinear photonic crystals. The nonlinear interaction between waves in these structures can be regarded as a scattering [4] process for which the efficient scattering of the signal wave is formulated as a momentum conservation law; it can be satisfied up to a reciprocal lattice vector (RLV) $\mathbf{G}$ of the photonic structure [5], so $\mathbf{G}=\mathbf{k_s}+\mathbf{k_i}-\mathbf{k_p}$. Different diffraction conditions (or QPM orders) are obtained by different RLV vectors.

The first modulation scheme to be studied was a 1D periodic QPM [1]. This simple modulation is limited for the efficient phase matching of a single nonlinear process. Therefore, numerous schemes of periodic and aperiodic photonic structures [6–13] were suggested for the complicated task of phase matching multiple nonlinear processes simultaneously. By these schemes, nonlinear cascading [14,15] can be realized, i.e., the output of one nonlinear process can be used as the input of a second nonlinear process. Cascading nonlinear processes enhance the possible applications that can be obtained by photonic structures, such as third-harmonic generation or polarization rotation.

The annular, periodically poled, nonlinear photonic structure [16,17] shown in Fig. 1(a) has received considerable attention lately. It is characterized by a continuous radial symmetry, but it possesses no translation symmetry. The function that represents the binary modulation of the nonlinear coefficient is $g(r)=\mathrm{sign}(\cos(2\pi r/\Lambda))$. Its spatial spectrum contains rings located at discrete radii of $q_n=2\pi\cdot n/\Lambda$. If the Ewald sphere [5] intersects with one of these rings the interaction is phase-matched. A very efficient collinear phase matching occurs if the phase mismatch $\Delta\mathbf{k}$ equals to $2\pi/\Lambda$, i.e., a first-order QPM. This process will be continuously phase-matched (because of radial symmetry) for each pump input angle.

It was shown that by transverse phase matching (TRPM) [19,20], the annular periodic structure supports the generation of second-harmonic (SH) conical waves or Bessel beams, which propagate within the nonlinear crystal and eventually evolve into rings at the far field. It was also shown that spatiotemporal toroidal waves can be generated in the annular periodic structure using counterpropagating ultrashort pump pulses.

Here we show that radial structures can be designed to support multiple processes for the purpose of cascading, nonlinear beam shaping, and nonlinear polarization switching. The periodic annular photonic structure that was recently investigated is only one specific example of a diverse family of radial photonic structures displayed in Fig. 1. The modulation of the nonlinear coefficient of these structures can be represented by

$$g(r,\varphi)=\Pi_{mn}[\mathrm{sign}(\cos(q_n\cdot r))\cdot\mathrm{sign}(\cos(m\cdot\varphi))], \quad (1)$$

where q_n is a set of spatial frequencies and m represents integers. Continuous radial symmetry structures shown in Fig. 1(a) and 1(b) generally may be represented by

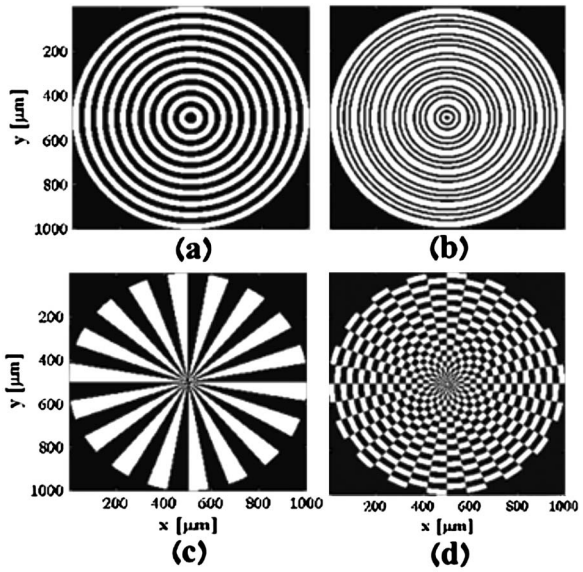

Fig. 1. Family of radial photonic structures. The black and white areas denote negative and positive signs of nonlinear coefficients, respectively. (a) Periodic annular photonic structure characterized by period Λ. (b) Aperiodic continuous radial photonic crystal characterized by several periods Λ_n. (c) Discrete periodic radial photonic crystal characterized by azimuthal angle φ. (d) Discrete periodic radial photonic crystal characterized by azimuthal angle φ and radial period Λ.

$g(r,\varphi)$ where $m=0$. Their spectra contain several rings spaced periodically or aperiodically. Up until now, only the periodic annular structure with continuous radial symmetry shown in Fig. 1(a) [16] has been discussed. Discrete radial structures shown in Fig. 1(c) and 1(d) can be represented by $g(r,\varphi)$. A special case is the "fan" structure shown in Fig. 1(c) where $q_n=0$. The spectra of the discrete structures contain azimuthally shaped intensity rings. The structure of Fig. 1(d) is a 2D, periodic, nonlinear photonic crystal in cylindrical coordinates, analogous to the 2D periodic structure in Cartesian coordinates [3,5,21]. It is worth noting that nonlinear devices possessing radial symmetry can also be realized using random, rather than ordered, structures. One recent realization was done [18] by randomly rotating a unit lattice of a 2D nonlinear photonic crystal.

We start our discussion in Section 2 by giving an example of cascading two nonlinear processes in radial structures. We analyze the generation of a radial third-harmonic wave in two different configurations—transverse and longitudinal QPM. In Section 3 we discuss potential applications of radial structures by longitudinal QPM. Generally they can be used for multidirectional third-harmonic generation or density shaping of noncollinear processes. We present a novel structure: a quasi-periodic radial structure. This structure possesses an important feature—it can be designed to support arbitrary nonlinear processes in any direction. In Section 4 we discuss applications of these structures in transverse QPM configurations such as multicolored rings, azimuthal or radial polarization shaping, etc. In Section 5 we analyze special polarization states of output waves in radial structures. We show that polarization effects must be taken into account when light waves interact in radially symmetric, nonlinear photonic crystals.

2. MULTIPLE PROCESSES WITH RADIAL SYMMETRY

There are numerous applications for phase matching multiple processes simultaneously that can be done longitudinally or transversely. We introduce the concept of phase matching multiple processes in radially symmetric structures by a common example of third-harmonic generation (THG).

Third-harmonic waves can be generated by cascading [14] two nonlinear processes. The first process is second-harmonic generation (SHG), where two pump photons with frequency ω are converted into one second-harmonic photon of frequency 2ω. The following process is when one photon of frequency ω and another photon of frequency 2ω convert by sum frequency generation (SFG) into one photon of frequency 3ω. For both of these processes we need a photonic structure that contains two RLVs—$\mathbf{G}_1=\mathbf{k}^{2\omega}-2\mathbf{k}^{\omega}$ and $\mathbf{G}_2=\mathbf{k}^{3\omega}-\mathbf{k}^{2\omega}-\mathbf{k}^{\omega}$.

We suggest two experimental ways to achieve radial THG. The first way is by longitudinal collinear QPM, when the pump beam propagates in the modulation plane as depicted in Fig. 2(a). For THG by longitudinal collinear

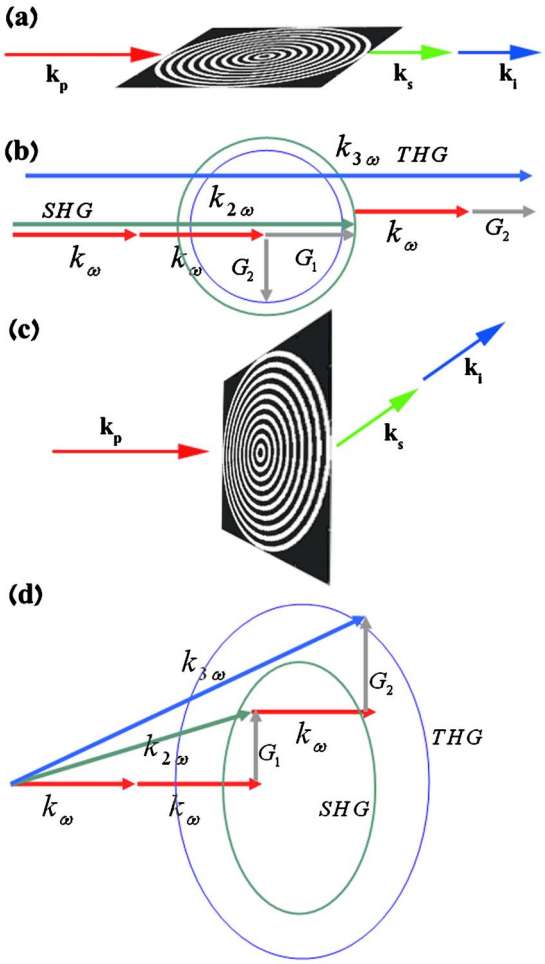

Fig. 2. (Color online) THG with continuous radial symmetry. (a) Longitudinal QPM; the pump beam propagates in the modulation plane. (b) Wave vector diagram for THG. (c) Transverse QPM; the pump beam is orthogonal to the modulation plane. (d) Wave vector diagram for simultaneous conical SHG and THG.

QPM, the RLVs are $|\mathbf{G}_{L1}|=|\mathbf{k}^{2\omega}|-2|\mathbf{k}^{\omega}|$ and $|\mathbf{G}_{L2}|=|\mathbf{k}^{3\omega}|-|\mathbf{k}^{2\omega}|-|\mathbf{k}^{\omega}|$. If the spectrum of the radial photonic structure contains rings with radii $|\mathbf{G_{L1}}|$ and $|\mathbf{G_{L2}}|$, THG can be obtained for each incidence angle of the pump beam as shown in Fig. 2(b).

TRPM is when the pump beam propagates orthogonally to the modulation plane as shown in Fig. 2(c). For THG by TRPM the spectrum of the structure should contain two RLVs:

$$|\mathbf{G}_{T1}| = \sqrt{|\mathbf{k}^{2\omega}|^2 - |2\mathbf{k}^{\omega}|^2},$$

$$|\mathbf{G}_{T2}| = \sqrt{|\mathbf{k}^{3\omega}|^2 - |3\mathbf{k}^{\omega}|^2} - |\mathbf{G}_{T1}|. \quad (2)$$

The output beams that result from these transverse processes are the SH cone wave and the TH cone wave as shown in Fig. 2(d). The transverse THG process is noncollinear and resembles by its geometry the 1D scheme of noncollinear THG [22], except that it is spanned radially. The spectrum of the radial structure should be designed to contain circles with the mentioned radii, which are generally incommensurate. This can be achieved by designing radial photonic structures (periodic or aperiodic) that are characterized by several radii as shown in Fig. 1(b).

3. LONGITUDINAL QUASI-PHASE MATCHING IN RADIAL STRUCTURES

A. Radial Phase-Reversed Structures

Generally each radial structure can be characterized by periods Λ_n and azimuthal angles φ_m. With these characteristics, the Fourier space of these structures can be engineered so that it contains rings with several arbitrary desired radii. In addition, the intensity of these rings can be azimuthally modulated.

We found that known 1D QPM modulation techniques can be applied to construct radial nonlinear photonic crystals that support multiple nonlinear processes simultaneously. Here we demonstrate this by a phase-reversed QPM technique [12]. However, it should be stressed that other modulation techniques, e.g., quasi-periodic [6,8] modulation, may be used as well.

A periodic 1D binary modulation function of the nonlinear coefficient $g(z)=\mathrm{sign}(\cos(2\pi z/\Lambda_{\mathrm{QPM}}))$ can be represented by its Fourier series, $g(z)=\sum_{m=-\infty}^{\infty}C_m\exp(iG_m\cdot z)$, where $C_m=\mathrm{sinc}(m\pi/2)$ and $G_m=2\pi/\lambda_{\mathrm{QPM}}$. In phase-reversed QPM a 1D QPM structure with period Λ_{QPM} is multiplied with another 1D QPM structure with period Λ_{phase}. Thus the phase-reversed structure can be represented by a multiplication of two series: $g(z)=\sum_{m,n=-\infty}^{\infty}C_{mn}\exp(iG_{mn}\cdot z)$, where $C_{mn}=\mathrm{sinc}(m\pi/2)\cdot\mathrm{sinc}(n\pi/2)$ and $G_{mn}=2\pi m/\Lambda_{\mathrm{QPM}}+2\pi n/\Lambda_{\mathrm{phase}}$.

A radial phase-reversed structure can be constructed in the same way. The binary function of the radial phase-reversed structure can be represented by $g(r)=\mathrm{sign}(\cos(2\pi r/\Lambda_{\mathrm{QPM}}))\cdot\mathrm{sign}(\cos(2\pi r/\Lambda_{\mathrm{phase}}))$, where the phase-reversed radial structure can be represented by Fourier series [23]

$$g(r) = \sum_{m,n=-\infty}^{\infty} C_{mn}\exp(iG_{mn}\cdot r),$$

$$C_{mn} \propto \mathrm{jinc}(m\pi/2)\cdot\mathrm{jinc}(n\pi/2),$$

$$G_{mn} = \frac{2\pi m}{\Lambda_{\mathrm{QPM}}} + \frac{2\pi n}{\Lambda_{\mathrm{phase}}}, \quad (3)$$

where $r=\sqrt{(x^2+y^2)}$, $\mathrm{jinc}(x)=J_1(x)/x$, and J_1 is a Bessel function of the first kind. We conclude that the spatial spectrum of the phase-reversed structure contains circles with different incommensurate radii G_{mn}. Thus, when $\Delta k=\sqrt{(k_x^2+k_y^2)}=G_{mn}$, several different interactions can be phase matched radially.

We further conclude that if one wants to phase match multiple processes with radial symmetry, all that needs to be done is to construct a 1D structure with peaks at the desired phase mismatch values and to span it radially.

We examined noncollinear phase-matching possibilities within Fourier spectra by Ewald constructed of several phase-reversed radial structures as presented in Fig. 3. Note that the studied cases are of longitudinal QPM SHG. When the Ewald sphere (phase mismatch circle) intersects with a circle on the Fourier space, the interaction is phase-matched. The walk-off angle ρ_{mn} between the pump and SH beam can be obtained by the law of cosines:

$$\cos(\rho_{mn}) = \frac{(2k^{\omega})^2 + (k^{2\omega})^2 - G_{mn}^2}{4k^{\omega}k^{2\omega}}. \quad (4)$$

We conclude that radial structures can be engineered so that they support multiple processes in various discrete noncollinear configurations as shown in Fig. 3. Whereas in the periodic annular structure, the different phase-matching orders (phase matched by different rings in the reciprocal lattice) are typically separated by large walk-off angles, in the phase-reversed radial structure the separation between the walk-off angle can be made very small (as shown in Fig. 3(c), where $\Lambda_{\mathrm{QPM}}\approx\Lambda_{\mathrm{phase}}$). As an example for doubling $\lambda=1.55$ μm, we can build a "dense" radial structure with periods: $\Lambda_{\mathrm{QPM}}=20.8$ μm and $\Lambda_{\mathrm{phase}}=16.6$ μm. The minimal domain resolution in such structure is ~ 4 μm. This feature is convenient for diagnostic properties of the crystal and the light beam, since all of these phase-matching orders are obtained simultaneously [16].

B. Phase Matching with Continuous Angular Symmetry

Radial photonic structures can be engineered to phase match multiple processes with various discrete noncollinear geometries. Noncollinear processes with continuous angular symmetry, i.e., phase matching for all directions, can be achieved by a different radial photonic structure. The structure is designed so its Fourier spectrum will contain the exact Ewald sphere (phase mismatch circle). This cannot be obtained with a simple radial structure, because the center of an Ewald sphere is shifted from the center of the Fourier space by the k vectors of the input waves ($2k^{\omega}$ in case of SHG). However, we can shift the circle in the reciprocal lattice by multiplying the structure by an appropriate phase in the real space. We define: $k_{\mathrm{shift}}=2k^{\omega}$, which represents the shift of the circle from the center of axis and $k_R=k^{2\omega}$, which represents the radius of the desired circle. The binary modula-

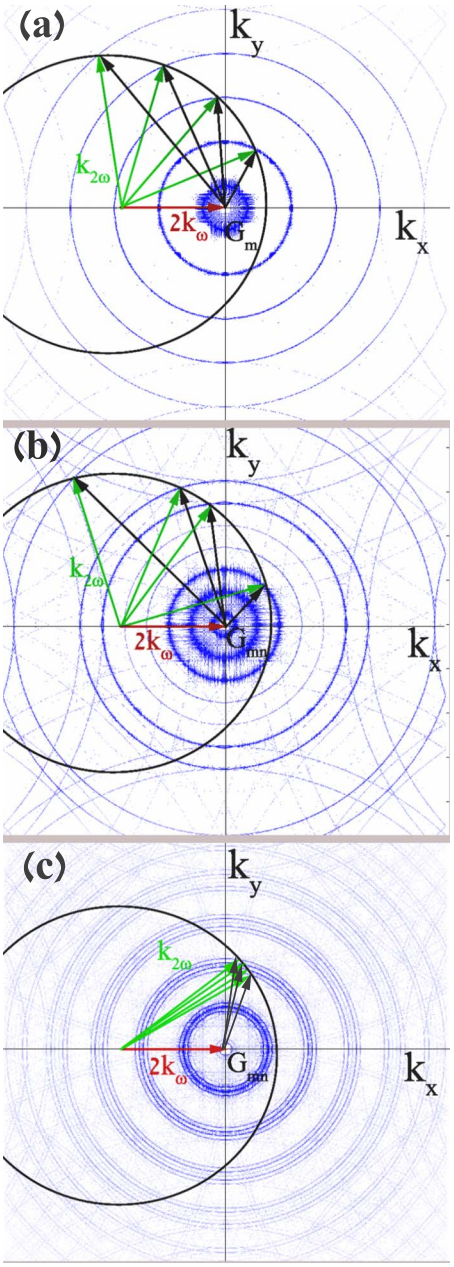

Fig. 3. (Color online) Density shaping of noncollinear processes by phase-reversed structures. Phase matching is obtained when the (black) circle (Ewald sphere) intersects with the (blue) circles (Fourier spectrum circles). (a) Periodic annular structure. The noncollinear processes are usually with large walk-off and they are hard to detect experimentally. (b) Phase-reversed structure $\Lambda_{\text{phase}}=3\cdot\Lambda_{\text{QPM}}$. (c) Phase reversed structure $\Lambda_{\text{QPM}}\approx\Lambda_{\text{phase}}$.

tion that represents such a structure in real space (shown in Fig. 4(b) is

$$d(x,y)=\text{sign}(\cos(x\cdot k_{\text{shift}}))\cdot\text{sign}(\cos(r\cdot k_R)). \quad (5)$$

The Fourier transform of this structure is shown in Fig. 4(a) is

$$D(k_x,k_y)=[\delta(k_x-k_{\text{shift}})+\delta(k_x+k_{\text{shift}})]\otimes F(k_R). \quad (6)$$

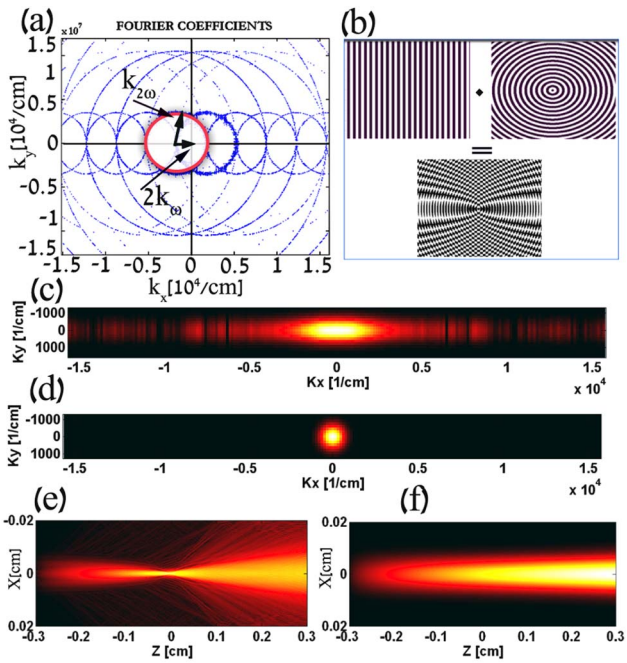

Fig. 4. (Color online) Phase matching with continuous angular symmetry. (a) Fourier spectrum of a photonic structure that supports phase matching for all directions. The Ewald construction (red) circle coincides with a circle (blue) upon the Fourier space. (b) Annular periodic photonic structure multiplied with 1D periodic structure. (c) Far-field simulation of SH beam at the crystal output. (d) Far-field simulation of SH beam at the crystal output in a 1D periodic structure. Note that the far-field image of the radial structure is wider than the far-field output of the 1D structure. (e) Scaled intensity of SH accumulated along the propagation path of the beams in z direction. (f) Scaled intensity of SH accumulated along the propagation path of the beams in z direction in a 1D periodic structure.

The Ewald construction coincides with a circle on the Fourier space; thus, the interaction is phase-matched for all propagation directions of the signal wave, with continuous angular symmetry. We simulated the aggregation of SH intensity along the propagation path of the beams within this photonic structure by a split-step Fourier numerical simulation in a stoichiometric lithium tantalate (SLT) [24]. The crystal's length and temperature were $L=0.6$ cm and $T=100\,^{\circ}\text{C}$, respectively. We used a Gaussian input beam with wavelength and waist of $\lambda=3.496$ μm and $\omega_0=60$ μm, respectively. The structure was designed by $k_R=7.5812\cdot10^6$ [1/m] and $k_{\text{shift}}=7.3763\cdot10^6$[1/m]. Fig. 4(e) represents a scaled SH intensity accumulation along the propagation path of the beam. Fig. 4(c) is the far field of the output SH beam. The results were compared with a propagating SH along a 1D (not annular) periodic nonlinear photonic crystal. In this case, the simulation parameters were: $L=0.6$ cm, $T=100\,^{\circ}\text{C}$, $\lambda=3.501$ μm, and $\omega_0=60$ μm. The structure was designed by: $k_x=2.0499\cdot10^5$ [1/m]. The propagating SH is displayed in Fig. 4(f). The conversion efficiency of this structure was $4.07\cdot10^{-5}$ [1/W] and in the 1D periodic case was $1.45\cdot10^{-4}$ [1/W]. It is clear that the action of phase matching for all directions has widened the SH intensity profile. However, the conversion efficiency was reduced. The construction of energy was still highest at the beam's center because of maximized interaction length. The two

simulations were operated with slightly different wavelengths because the maximal efficiency point is slightly differently for each structure.

C. Quasi-periodic Radial Photonic Structure

Quasi-periodic structures are ordered, nonperiodic structures whose reciprocal lattice contains at least two incommensurate frequencies. Quasi-periodic 1D modulation of the nonlinear coefficient was previously used to simultaneously phase match several arbitrary collinear nonlinear processes [6,8]. Later it was shown that efficient 2D nonlinear photonic quasi-crystals can phase match arbitrary processes in chosen discrete directions by the dual grid method (DGM) [25]. The degree of freedom in this case is in the lateral movement for which the geometry that the pump beam experiences is unchanged under lateral translation. Since the interaction occurs with a beam of finite width, this degree of freedom is not critical. We suggested a different way to phase match arbitrary nonlinear processes in any direction (which are not fixed) by radially symmetric, nonlinear photonic quasi-crystals. By this configuration we gain an important feature: arbitrary processes can be phase-matched for all pump input angles (with radial symmetry). However, we lose the lateral translation symmetry since the input beams must pass through the center of the radial structure.

A quasi-periodic radial photonic structure is schematically presented in Fig. 5(a). It contains concentric rings with radii given by a quasi-periodic sequence. This quasi-periodic radial photonic structure can support any set of arbitrary nonlinear processes in a radial fashion (for all pump input angles).

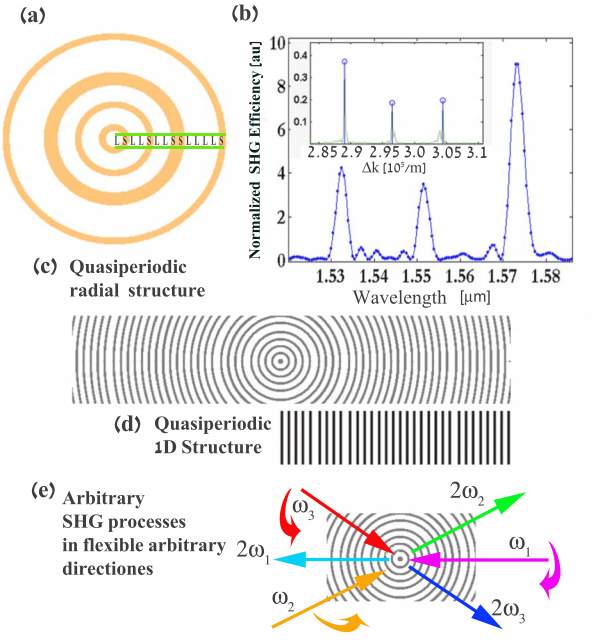

Fig. 5. (Color online) Phase matching arbitrary multiple processes in any direction by radial nonlinear photonic quasi-crystal. (a) Quasi-periodic radial nonlinear photonic crystal (b) Numerical simulation results of SH efficiency of radial photonic structure (shown in the inset) that supports three nonlinear process of 1.53, 1.55, and 1.57 μm simultaneously. This phase matching applies for each input angle of pump beam, i.e., with radial symmetry. (inset) The Fourier coefficients of the source 1D quasi-periodic structure. (c) Nonlinear radial quasi-periodic structure spanned from 1D quasi-periodic structure (d) that was constructed by DGM. (e) Scheme of phase matching arbitrary processes in any direction.

To illustrate its features we constructed a radial quasi-crystal that phase matches three arbitrary processes. We first designed a 1D quasi-crystal in Fig. 5(d) by DGM, which longitudinally phase matches three SHG processes of 1.53, 1.55, and 1.57 μm [26]. The phase mismatches of SHG in SLT are 3.0467, 2.9673, and 2.8927 $[10^5/\mathrm{m}]$, respectively. The structure's building blocks were 6.87, 7.23, and 7.47 μm. The duty cycles were 0, 1, and 0, respectively. Fourier coefficients of the 1D structure are shown in the inset of Fig. 5(b) (x axis represents spatial frequencies in $[10^5/\mathrm{m}]$ and y axis represents the Fourier coefficients.) Then it was spanned radially as shown in Fig. 5(c).

We simulated the efficiency of SHG in the radial structure by using the Fourier split-step method. The simulation parameters were: $L=0.5$ cm, $T=25°\mathrm{C}$, and $\omega_0=20$ μm. The simulation results are presented in Fig. 5(b). The conversion efficiencies for the three processes where $3.45\cdot10^{-4}$, $3.4\cdot10^{-4}$, and $6.5\cdot10^{-4}$ [1/W], respectively. These efficiencies were very similar to the efficiencies of a 1D quasi-periodic structure: $2.8\cdot10^{-4}$, $3.8\cdot10^{-4}$, and $6.1\cdot10^{-4}$ [1/W], respectively. The similarity of the results is because a narrow stripe of a radial structure resembles a 1D structure. The quasi-periodic structure efficiently supports all three processes. This result is significant since phase matching of several arbitrary processes can be obtained efficiently for any pump input angles, as illustrated in Fig. 5(e). This structure may be placed inside a ring resonator. Its rich spectrum can phase match multiple different processes, and its radial symmetry can facilitate the planning of the resonator's geometrical configuration.

4. TRANSVERSE QUASI PHASE MATCHING IN VARIOUS GEOMETRIES

In this section we present several applications of radial structures that can be realized by TRPM. The first application is the multicolored SH rings visualized in Fig. 6(a). This application can be realized by structures similar to the one shown Fig. 1(b). Each SH ring results from a different diffraction condition and thus appears with a different radius.

We simulated transverse QPM on a phase-reversed radial structure that was constructed to support two transverse radial SH processes of 1500 nm and 1600 nm. The results are presented in Fig. 6(b) and 6(c). We simulated the far-field output image of SH for each peak as shown in Fig. 6(d). We got different rings for each wavelength. There is also a possibility to plan a chirped radial structure that phase matches a range of processes and thus generates adjustable and all optically controlled SH rings [27].

By using structures similar to the one shown Fig. 1(d), we can shape azimuthally the intensity of the SH rings. The output rings will be similar to the one shown in Fig. 6(e). By inserting a light beam into a structure shown in Fig. 1(c) (the "fan" structure), we can design a multicolored star beam.

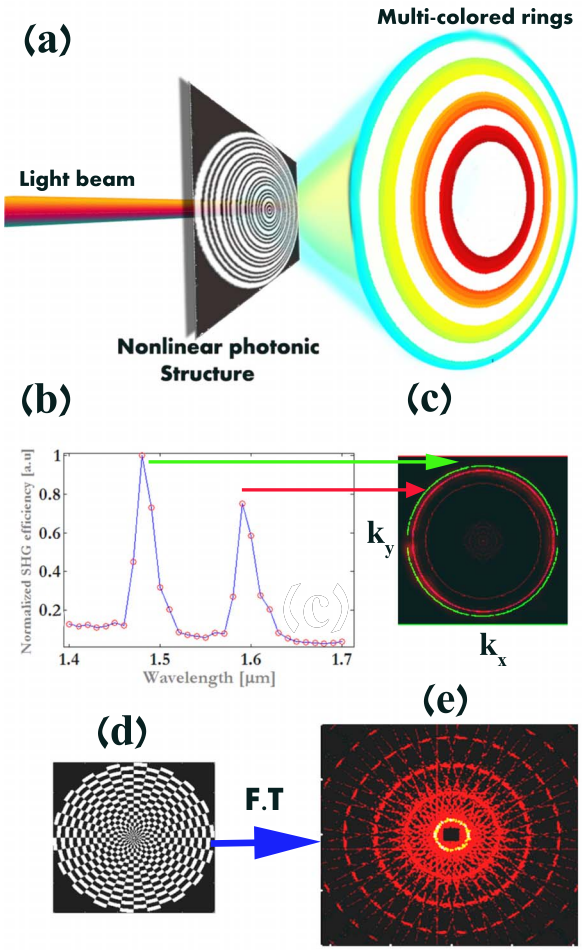

Fig. 6. (Color online) Applications of radial photonic crystals by transverse QPM. (a) Multicolored rings scheme. Each colored ring results from a different diffraction condition. (b) Simulation results of the efficiency of phase-reversed structure that supports transverse phase matching of 1500 nm and 1600 nm. (c) Simulated far-field output of each process–two SH rings of different colors. (d) Discrete radial structure for azimuthal intensity shaping. (e) Azimuthal intensity shaping of SH rings.

5. POLARIZATION STATES IN RADIAL SYMMETRY INTERACTIONS

In order to fully describe nonlinear interactions within radially symmetric structures, we need to take into account the polarization states of the generated waves that essentially affect the efficiency of interactions and shape the generated beams [20]. We will use this section to analyze the polarization effects on single and cascaded three-wave mixing processes with radial symmetry for longitudinal and transverse phase-matching configurations. We analyze in the following section the generated polarization states for crystals that belong to the 3 m symmetry point group, e.g., $LiNbO_3$ and $LiTaO_3$.

A. Polarization States for Longitudinal Phase Matching

For longitudinal phase-matching configuration, as shown on Fig. 2(a), extraordinary waves polarized in the z direction and ordinary waves polarized in the x–y plane can be generated by [e-oo] or [e-ee] and [o-oo] or [o-eo] interactions, respectively. In this configuration, the polarization of extraordinary waves generated by [e-oo] or [e-ee] interactions will always be perpendicular to the propagation direction of the waves; thus, the efficiency of generation is isotropic.

However, for [o-eo] and [o-oo] the generated polarization will be in the plane of propagation, and the efficiency of interactions will have azimuthal dependence. This dependence rises from the fact that the locally generated polarization, i.e., the polarization of the SH wave is determined by the symmetry point group, while the polarization of the propagating SH field is determined by the propagation direction, which is set by phase-matching conditions. Only the projection of the locally generated polarization on the plan normal to $\mathbf{k}_{2\omega}$ will contribute to the total generated efficiency [28]. Thus, when constructing a structure with continuous radial symmetry, which is supposed to collinearly phase match (one process or more) for all pump incidence angles as described above, we need to modify the analysis and to take into account that the efficiency of [o-eo] and [o-oo] interactions is azimuthally dependent.

For [o-eo] interactions the projection factor of the locally generated field on the propagating field can be calculated to be $\cos(\rho)$, where ρ is the angle between the wave vector of the ordinary pump wave $\mathbf{k}_{\omega}$ and the wave vector of the ordinary generated wave $\mathbf{k}_{2\omega}$, and it is determined by the phase-matching conditions. Considering this relationship, we can understand, for instance, that it is not possible to use the [o-eo] interaction to generate waves that travel in perpendicular directions to the ordinary pump wave, even when using structures that support the phase mismatch in these directions, e.g., structures shown on Fig. 3 and Fig. 4(b).

For the case of [o-oo] interactions, the local polarization of the generated ordinary waves will have the form of $\vec{P}_{\text{local}} = \sin(2\gamma)\hat{x} + \cos(2\gamma)\hat{y}$ as shown on Fig. 7(a), and the projection factor will be $\sin(3\gamma + \rho)$. This relation sets an azimuthal transparency window for the generated waves, which has to be taken into account when considering longitudinal [o-oo] interactions. Fig. 7(b) shows the effect of the azimuthal transparency window in generating THG with continuous radial symmetry that is based on ordinary interactions. We can actually learn about the symmetry group of an unknown crystal by poling it radially and measuring its azimuthal transparency window.

B. Polarization States of Transverse Phase Matching

We assume that, owing to the relatively small propagation angles, interactions involving d_{33} and d_{31} can be neglected [20]. However, polarization states of [o-oo] interactions (using the d_{22} element of the $\chi^{(2)}$ tensor) at transverse phase-matching configurations show unique and interesting properties. As in the case of longitudinal phase matching, the local generated polarization of the second-harmonic wave will have the form of $\vec{P}_{\text{local}} = \sin(2\gamma)\hat{x} + \cos(2\gamma)\hat{y}$, which sets an angle of $\pi/2 - 2\gamma$ counterclockwise to the x direction. If we now consider sum frequency generation of two pump beams with different angles of polarizations γ_1 and γ_2, the local generated polarization will have an angle of $\pi/2 - \gamma_1 - \gamma_2$. Using these relations we can understand that a polarization rotation of the generated waves will occur for $\gamma = m\pi/3$, and that

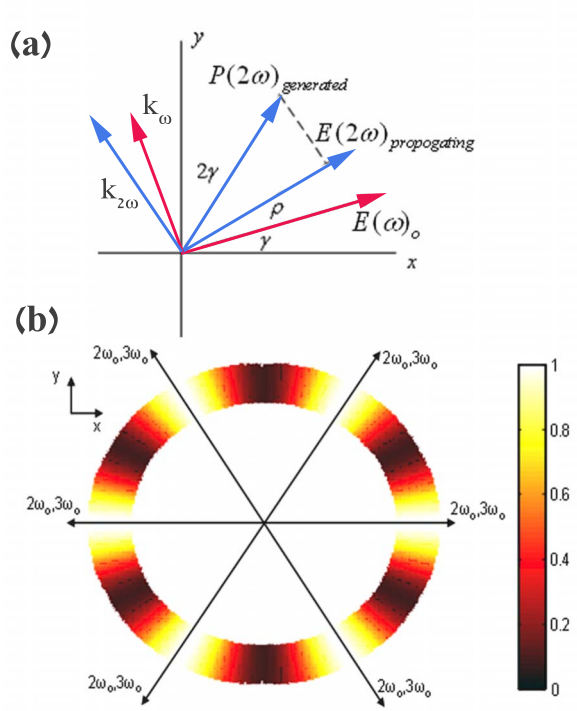

Fig. 7. (Color online) Azimuthal transparency window for [o-oo] interactions. (a) Polarization and propagation directions of interacting waves in [o-oo] interactions. The polarization of SH generated wave is $\vec{P}_{local}=\sin(2\gamma)\hat{x}+\cos(2\gamma)\hat{y}$. The projection of the generated polarization onto the direction of the propagating wave is $\sin(3\gamma+\rho)$. (b) Transparency window for longitudinal THG with continuous radial symmetry using [o-oo] interactions for 3 m symmetry point group crystals.

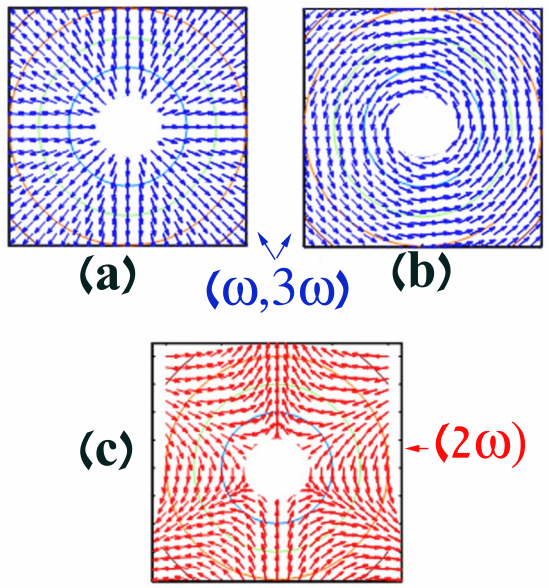

Fig. 8. (Color online) Special polarization states by transverse QPM in radial structures. (a) and (b) Radial and azimuthal polarization states of pump beams, respectively. (c) Generated $\pi/2-2\varphi$ polarization state of the SH for both pump polarization states (radial or azimuthal) shown in (a) and (b). In case of THG the TH wave will maintain the polarization state of the pump.

equally polarized generation will occur for $\gamma=\pi/6+m\pi/3$. A cascaded interaction, e.g., SHG and THG, will result in the following angels (Γ) of polarization states for the generated beams:

$$\Gamma_{SH}(\Gamma_{pump}=\gamma)=\pi/2-2\gamma, \tag{7}$$

$$\Gamma_{TH}(\Gamma_{pump}=\gamma,\Gamma_{SH}=\pi/2-2\gamma)=\pi/2-\gamma-(\pi/2-2\gamma)=\gamma. \tag{8}$$

It is also interesting to examine the states of polarizations generated by radially symmetric beams, e.g., radially polarized beams [see Fig. 8(a)] or azimuthally polarized beams [Fig. 8(b)], when using radially symmetric structures in transverse configurations. For small angle interactions the SH waves in both cases will have the same azimuthal polarization dependence, $\pi/2-2\varphi$, as shown in Fig. 8(c) where φ is the azimuthal angle with respect to the x direction. However in a cascaded interaction the TH wave will gain back the polarization state of the pump wave, i.e., a radial pump will generate a radial TH wave, and an azimuthal pump will generate an azimuthal TH wave.

6. SUMMARY AND CONCLUSIONS

We have presented a new family of nonlinear photonic structures having either continuous or discrete radial symmetry. Their symmetry is useful for phase matching nonlinear interactions in any direction. Moreover, aperiodic radial modulations enable us to simultaneously phase match multiple wavelength interactions. It was shown that the density of noncollinear processes can be shaped by constructing a crystal with an appropriate Fourier spectrum.

We have discussed the possibility of continuous angular phase matching (for all directions) by designing a structure spectrum that contains an exact Ewald sphere. Numerical simulation showed that even though the SH was phase matched for all directions, it was built very efficiently in the collinear direction due to longer, effective interaction length. We have proposed schemes for constructing multiwavelength converters, multicolored rings, and azimuthal beam shaping using phase-reversed or quasi-periodic modulation in radial coordinates. These devices can be used for generating multiple harmonics in arbitrary directions.

Finally, we have shown that polarization effects must be taken into account (especially for [o-oo] interactions) and that interactions in a continuous radial structure can be spatially dependent. We have discussed interesting polarization states of beams generated in radial structures and have shown that polarization states can be shaped in radially symmetric structures.

This work was partially supported by the Israeli Science Foundation grant 960/05 and by the Ministry of Science, Culture, and Sports.

REFERENCES

1. M. M. Fejer, G. A. Magel, D. H. Jundt, and R. L. Byer, "Quasi-phase-matched second harmonic generation-tuning

and tolerances," IEEE J. Quantum Electron. **28**, 2631–2654 (1992).
2. M. Yamada, N. Nada, M. Saitoh, and K. Watanabe, "First-order quasi-phase matched $LiNbO_3$ waveguide periodically poled by applying an external field for efficient blue second-harmonic generation," Appl. Phys. Lett. **62**, 435–436 (1993).
3. N. G. R. Broderick, G. W. Ross, H. L. Offerhaus, D. J. Richardson, and D. C. Hanna, "Hexagonally poled lithium niobate: a two-dimensional nonlinear photonic crystal," Phys. Rev. Lett. **84**, 4345–4348 (2000).
4. I. Freund, "Nonlinear diffraction," Phys. Rev. Lett. **21**, 1404–1406 (1968).
5. V. Berger, "Nonlinear photonic crystals," Phys. Rev. Lett. **81**, 4136–4139 (1998).
6. S. N. Zhu, Y. Y. Zhu, and N. B. Ming, "Quasi-phase-matched third-harmonic generation in a quasi-periodic optical superlattice," Science **278**, 843–846 (1997).
7. H. Liu, S. N. Zhu, Y. Y. Zhu, N. B. Ming, X. C. Lin, W. J. Ling, A. Y. Yao, and Z. Y. Xu, "Multiple-wavelength second-harmonic generation in aperiodic optical superlattices," Appl. Phys. Lett. **81**, 3326–3328 (2002).
8. K. Fradkin, A. Arie, P. Urenski, and G. Rosenman, "Multiple nonlinear optical interactions with arbitrary wave vector differences," Phys. Rev. Lett. **88**, 023903 (2001).
9. J. Liao, J. L. He, H. Liu, J. Du, F. Xu, H. T. Wang, S. N. Zhu, Y. Y. Zhu, and N. B. Ming, "Red, yellow, green and blue four-color light from a single, aperiodically poled $LiTaO_3$ crystal," Appl. Phys. B **78**, 265–267 (2004).
10. R. Lifshitz, A. Arie, and A. Bahabad, "Photonic quasicrystals for nonlinear optical frequency conversion," Phys. Rev. Lett. **95**, 133901 (2005).
11. R. T. Bratfalean, A. C. Peacock, N. G. R. Broderick, K. Gallo, and R. Lewen, "Harmonic generation in a two-dimensional nonlinear quasi-crystal," Opt. Lett. **30**, 424–426 (2005).
12. M. H. Chou, K. R. Parameswaran, M. M. Fejer, and I. Brener, "Multiple-channel wavelength conversion by use of engineered quasi-phase-matching," Opt. Lett. **24**, 1157–1159 (1999).
13. M. Baudrier-Raybaut, R. Haïdar, Ph. Kupecek, Ph. Lemasson, and E. Rosencher, "Random quasi-phase-matching in bulk polycrystalline isotropic nonlinear materials," Nature (London) **432**, 374–376 (2004).
14. G. I. Stegeman, D. J. Hagan, and L. Torner, "$\chi^{(2)}$ cascading phenomena and their applications to all-optical signal processing, mode-locking, pulse compression and solitons," Opt. Quantum Electron. **28**, 1691–1740 (1996).
15. Y. S. Kivshar, A. A. Sukhorukov, and S. M. Saltiel, "Two-color multistep cascading and parametric soliton-induced waveguides," Phys. Rev. E **60**, R5056–R5059 (1999).
16. D. Kasimov, A. Arie, E. Winebrand, G. Rosenman, A. Bruner, P. Shaier, and D. Eger, "Annular symmetry nonlinear frequency converters," Opt. Express **14**, 9371–9376 (2006).
17. T. Wang, B. Ma, Y. Sheng, P. Ni, B. Cheng, and D. Zhang, "Large-angle acceptance of quasi-phase-matched second-harmonic generation in homocentrically poled LiNbO3," Opt. Commun. **252**, 397–401 (2005).
18. Y. Sheng, J. Dou, J. Li, D. Ma, B. Cheng, and D. Zhang, "Broadband efficient second harmonic generation in media with a short-range order," Appl. Phys. Lett. **91**, 101109 (2007).
19. S. M. Saltiel, D. N. Neshev, R. Fischer, W. Krolikowski1, A. Arie, and Y. S. Kivshar, "Spatiotemporal toroidal waves from the transverse second-harmonic generation," Opt. Lett. **33**, 527–529 (2008).
20. S. M. Saltiel, D. N. Neshev, R. Fischer, W. Krolikowski1, A. Arie, and Y. S. Kivshar, "Generation of the second-harmonic conical waves via nonlinear Bragg diffraction," Phys. Rev. Lett. **100**, 103902 (2008).
21. A. Arie, N. Habshoosh, and A. Bahabad, "Quasi phase matching in two-dimensional nonlinear photonic crystals," Opt. Quantum Electron. **39**, 361–375 (2007).
22. T. Ellenbogen, A. Arie, and S. M. Saltiel, "Noncollinear double quasi-phase matching in one-dimensional poled crystals," Opt. Lett. **32**, 262–264 (2007).
23. I. Amidror, "Fourier spectrum of radially periodic images," J. Opt. Soc. Am. A **14**, 816–826 (1997).
24. A. Bruner, D. Eger, M. B. Oron, P. Blau, M. Katz, and S. Ruschin, "Temperature-dependent Sellmeier equation for the refractive index of stoichiometric lithium tantalate," Opt. Lett. **28**, 194–196 (2003).
25. A. Bahabad, A. Ganany-Padowicz, and A. Arie, "Engineering two-dimensional nonlinear photonic quasi-crystals," Opt. Lett. **33**, 1386–1388 (2008).
26. A. Bahabad, N. Voloch, A. Arie, and R. Lifshitz, "Experimental confirmation of the general solution to the multiple-phase-matching problem," J. Opt. Soc. Am. B **24**, 1916–1921 (2007).
27. T. Ellenbogen, A. Ganany, and A. Arie, "Nonlinear photonic structures for all-optical deflection," Opt. Express **16**, 3077–3082 (2008).
28. B. E. A. Saleh and M. C. Teich, *Fundamentals of Photonics* 2nd ed. (Wiley, 2007), Chap. 6.